East European Journal of Physics. **4.** 143-151 (2024)
DOI:10.26565/2312-4334-2024-4-13 ISSN 2312-4334

RADIATIVE EFFECT ON AN UNSTEADY DARCY FORCHHEIMER MHD FLOW OVER A VERTICALLY INCLINED STRETCHING SHEET IN PRESENCE OF POROUS MEDIUM

Ankur Kumar Sarma[a,e]*, Sunmoni Mudoi[a], Palash Nath[b], Pankaj Kalita[c], Gaurab Bardhan[d]
[a]*Department of Mathematics, Cotton University, Pan Bazaar, Guwahati-781001, India*
[b]*Department of Mathematics, Barbhag College, Kalag-781351, India*
[c]*Department of Mathematics, ADP College, Nagaon-782002, India*
[d]*Department of Mathematics, Tyagbir Hem Baruah College, Jamugurihat, Sonitpur, 784189, India*
[e]*Department of Mathematics, Baosi Banikanta Kakati College, Nagaon, Barpeta-781311, India*
**Corresponding Author e-mail: ankurkumarsarma44@gmail.com*
Received June 1, 2024; revised September 19, 2024; accepted September 29, 2024

This study looks at how radiation and heat move through a two-dimensional, unsteady Darcy-Forchheimer MHD flow that flows across a porous, stretched plate that is vertically inclined and has a transverse magnetic field applied to it. We use the MATLAB bvp4c approach to numerically translate the controlling boundary layer nonlinear PDEs, which are partial differential equations, into a set of nonlinear ODEs, which are ordinary differential equations, using the similarity transformation. We quantitatively assess the velocity and temperature profiles using graphs that represent the problem's various characteristics, including unsteadiness, Prandtl number, magnetic, Grashoff number, radiation parameter, and Eckert number. Tables illustrate the effects on skin friction (τ) and Nusselt number (Nu). The velocity profile decreases as the magnetic and inertial parameters increase, and the temperature profile decreases with the increases in the radiation parameters.
Keywords: *Magnetohydrodynamics (MHD); Radiation; Darcy-Forchheimer; Porous medium; Heat transfer; Unsteady*
PACS: 47.55.P-, 44.25.+f, 44.05.+e, 47.11.-j, 44.20.+b, 47.56.+r

INTRODUCTION

The study of magnetohydrodynamics (MHD) examines how magnetic fields affect the behavior of electrically conducting fluids, such as liquid metal and plasmas. This transdisciplinary area of study examines how fluid motion produces electric currents, which in turn produce magnetic fields that interact with the fluid by fusing concepts from electromagnetism and fluid dynamics. Applications for MHD may be found in geophysics, engineering, and astrophysics. In astrophysics, it explains phenomena like solar flares and star formation. In geophysics, it helps with the understanding of Earth's magnetic field and magnetospheric dynamics. MHD is crucial for researching phenomena ranging from space weather to industrial processes because of its intricate nonlinear equations regulating fluid motion, electric currents, and magnetic fields.

Any substance with holes or pores in it that let liquids through is called a porous media. These materials can be manufactured, like ceramics and foams made for certain uses, or they can be natural, like soils, rocks, and biological tissues. Numerous disciplines, including geology, hydrology, petroleum engineering, environmental science, and biomedical engineering, depend heavily on the study of fluid flow through porous media. The link between the fluid velocity and the pressure gradient inside the porous medium is described by Darcy's law, which controls the behavior of fluids in porous media. Fluid flow characteristics are influenced by variables including porosity (the percentage of empty space in the medium), permeability (a measure of how readily fluids may flow through the medium), and tortuosity (the increase in route length caused by obstructions). Porous media are useful in many different contexts. They have an impact on soil and aquifer contamination transfer as well as groundwater flow in hydrology. Understanding fluid movement through reservoir rocks is essential to petroleum engineering in order to maximize the extraction of oil and gas. Porous scaffolds are utilized in biomedical engineering to enhance cell development and enable waste and nutrition exchange in tissue engineering. Complicated mathematical and numerical simulations are frequently used to model fluid flow in porous media in order to forecast characteristics including fluid distribution, transport phenomena, and filtration procedures. Comprehending and refining these procedures is crucial in addressing pragmatic issues pertaining to resource allocation, environmental restoration, and technological progress.

Fluid motion in a porous material when viscous and inertial effects are important is described by Darcy-Forchheimer flow. In order to account for non-linear flow behavior at higher velocities or through extremely porous materials, it adds a term to Darcy's law. The resistance resulting from inertial forces is represented by the Forchheimer term in this model, and it becomes dominant as fluid velocities rise or the porosity of the porous medium increases. This phrase usually contains coefficients pertaining to the fluid density and viscosity, as well as the permeability and porosity of the medium. In order to represent fluid flow in porous tissues or scaffolds, Darcy-Forchheimer equations are used in a variety of domains, including groundwater hydrology, petroleum reservoir engineering, filtration processes, and biomedical engineering. Comprehending Darcy-Forchheimer flow is essential for precise fluid dynamics prediction and process optimization when fluid flow through porous media is important.

Cite as: A.K. Sarma, S. Mudoi, P. Nath, P. Kalita, G. Bardhan, East Eur. J. Phys. 4, 143 (2024), https://doi.org/10.26565/2312-4334-2024-4-13

The flow field resulting from a continuous surface flowing at a constant speed was established by Saikiadis [1]. He [2] then examined the flow of fluid across a continuous, flat surface. Crane [3] examined the flow and heat transmission across a stretched sheet of an electrically conducting viscous fluid's boundary layer. Boundary-layer equations for flow driven exclusively by a stretched surface were introduced and studied by Banks [4]. Numerous scientists study radiation and transverse magnetic field effects, realizing the benefits of using MHD to solve a wide range of technical issues and natural phenomena. Wang [5] then looked at the flow that an expanded flat surface produced in three dimensions. A perfect similarity solution was discovered via the Navier-Stokes equations. The fluid motion arising from the expansion of a flat surface was represented in three dimensions by the solution. Viscoelastic fluid flow over a stretched sheet in the presence of a transverse magnetic field was investigated by Andersson [6]. Viscoelasticity is shown to affect flow in a manner akin to that of an external magnetic field by providing an accurate analytical solution to the governing non-linear boundary layer equation. Elbashbeshy [7] investigated how injection and suction affected heat transport across a stretched surface with a constant and fluctuating surface heat flux. Furthermore, in the presence of suction, Siri et al. [8] investigated heat transfer across a continuous stretched surface. Researchers Andersson et al. [9] looked at how a horizontal sheet affected the heat transmission in a liquid film. Researchers Raptis et al. [10], Ghaly [11], Ishak et al. [12], and a few others evaluated the effect of heat radiation on MHD flow problems using a stretched sheet. Ariel [13] investigated the effects of axisymmetric stretching on boundary layer flows using the Homotopy perturbation method. The behavior of an incompressible fluid passing through a stretched surface in an unstable boundary layer with a heat source present was studied by Elbashbeshy et al. [14]. The increasing velocity associated with the surface and the time dependency of the heat flux lead to the instability of the temperature and flow fields. The mobility of the boundary layer and heat transfer across an extended plate with variable thermal conductivity were examined by Ahmad et al. [15]. Heat transmission via a stretched plate in combination with unstable MHD laminar flow was also studied by Ishak et al. [16]. Expanding on Ishak's work, Jhankal et al. [17] studied the stretched plate in the presence of a porous material. Research on the issue of unstable viscous flow on a curved surface was done by Natalia Rosca et al. [18]. In order to account for a transverse magnetic field of constant intensity, Choudhary et al. [19] conducted a theoretical study to explain a 2-dimensional unsteady flow over a stretched permeable surface of a viscous, incompressible electrically conducting fluid. Alarifi et al. [20] looked at the source influence as well as the MHD flow across a vertically extending sheet. When thermal radiation, fluctuating heat flow, and porous media are present, the MHD fluid movement generated by a stretched sheet that is not constant is examined by Megahed et al. [21]. The effects of a porous media on the flow of MHD heat transfer fluid across a stretched cylinder were examined by Reddy et al. [22]. The effect of thermal radiation on convective heat transport in Carreau fluid was examined by Shah et al. [23].

Rasool et al. [24] used the Darcy-Forchheimer relationship to investigate the Casson-type MHD nanofluid flow that occurred on a nonlinear stretching surface. Patil et al. [25] did a study on unstable mixed convection over an exponentially stretched surface. They looked at the effects of cross diffusion and the Darcy-Forchheimer porous medium. Al-Kouz et al. [26] explored MHD Darcy-Forchheimer nanofluid flow and entropy optimization in an atypically shaped container filled with MWCNT-Fe3O4/water. They did this by using Galerkin finite element analysis. Mandal et al. [27] studied the steady two-dimensional laminar mixed convective flow, heat transfer, and mass transfer for a Newtonian fluid that conducts electricity but not very well on an isothermal stretched semi-infinite inclined plate in a Darcy porous medium. Recent years have seen a number of researchers [28-30] focusing their attention on the investigation of Darcy-Forchheimer MHD flow with a variety of flow effects.

The work by Ishak at al. [16] is generalised in this paper. We have examined the problem of 2D, laminar flow that is unstable when radiation and a transverse magnetic field occur across a vertically inclined porous stretching plate in a Darcy Forchheimer MHD flow.

MATHEMATICAL FORMULATION

We investigate the flow of a porous vertically stretched plate inclined at an angle α with the vertical across an unstable, laminar, 2D MHD boundary layer flow in the presence of heat radiation. It's a viscous incompressible fluid that conducts electricity. The Hall effect and the polarization of charges are neglected. Externally applied transverse magnetic field B_0 is perpendicular to the x-axis in the positive direction of the y-axis. While the x-axis is parallel to the stretching plate, the y-axis is normal to it. The origin is held fixed as the surface is extended along the x-axis with a velocity of $U_w = \frac{ax}{1-ct}$. The problem is formulated in presence of radiation and Joule's heating [24] effect which has been incorporated in the energy equation (3). The graphical representation of the problem is depicted in Figure 1.

Under these conditions and Boussinesq's approximation, the governing continuity, momentum and energy equations [16][29] are:

$$\frac{\partial u}{\partial x} + \frac{\partial v}{\partial y} = 0, \tag{1}$$

$$\frac{\partial u}{\partial t} + u\frac{\partial u}{\partial x} + v\frac{\partial u}{\partial y} = \nu\frac{\partial^2 u}{\partial y^2} - \frac{\sigma_e B_0^2 u}{\rho} + g\beta(T - T_\infty)cos\alpha - \frac{\nu u}{k} - \frac{k'}{\sqrt{k}}u^2, \tag{2}$$

$$\frac{\partial T}{\partial t} + u\frac{\partial T}{\partial x} + v\frac{\partial T}{\partial y} = \frac{\kappa}{\rho C_p}\frac{\partial^2 T}{\partial y^2} + \frac{\sigma_e B_0^2 u^2}{\rho C_p} - \frac{1}{\rho C_p}\frac{\partial q_r}{\partial y}. \tag{3}$$

by virtue of boundary conditions [16] given by:

$$y=0: \quad u=U_w, \quad v=0, \quad T=T_w, \quad \text{and}$$

$$y\to\infty: \quad u\to 0, \quad T\to T_\infty, \tag{4}$$

q_r [12][30] is expressed as follows

$$q_r=-\frac{4\sigma_1}{3k_1}\frac{\partial T^4}{\partial y}, \tag{5}$$

where α indicates Stefan-Boltzmann constant, k_1 represents Rosseland mean absorption coefficient.

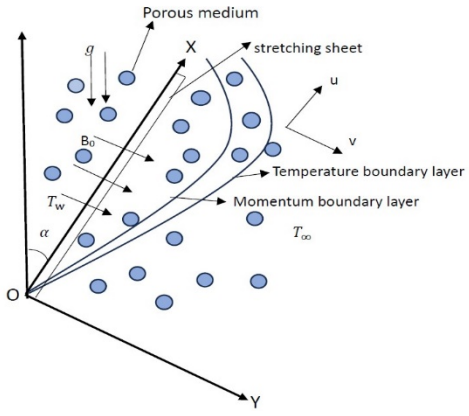

Figure 1. Graphical representation of the problem

Assuming that the difference in internal flow temperature is appropriately small, T^4 may be represented by the Taylor series around T_∞, omitting the components of higher order.

$$T^4=4T_\infty^3T-3T_\infty^4. \tag{6}$$

We consider the extending velocity $U_w(x,t)$ and surface temperature $T_w(x,t)$ are as follows:

$$U_w=\frac{ax}{1-ct}, \quad T_w=T_\infty+\frac{bx}{1-ct}. \tag{7}$$

Continuity equation (1) is fulfilled, by using a stream function ψ such that $u=\frac{\partial\psi}{\partial y}$ and $v=-\frac{\partial\psi}{\partial x}$.

The given nonlinear PDEs (2)- (3) are transformed to a set of nonlinear ODEs using following similarity variables and nondimensional quantities given as follows:

$$\eta=\left(\frac{a}{\nu(1-ct)}\right)^{\frac{1}{2}}y, \quad \psi=\left(\frac{a\nu x^2}{(1-ct)}\right)^{\frac{1}{2}}f(\eta), \quad \theta(\eta)=\frac{T-T_\infty}{T_w-T_\infty}, \quad A=\frac{c}{a}.$$

$$M=\frac{\sigma_eB_0^2(1-ct)}{\rho a}, \quad S_p=\frac{\nu(1-ct)}{ka}, \quad Ec=\frac{\mathrm{U_w^2}}{\mathrm{C_p(T_w-T_\infty)}}, F=\frac{k'}{\sqrt{k}},$$

$$N=\frac{\kappa k_1}{4\sigma_1T^3{}_\infty}, \quad \lambda=\frac{4+3N}{3N}, \quad Pr=\frac{\mu C_p}{\kappa}, \quad Gr=\frac{g\beta(1-ct)^2(T_w-T_\infty)}{a^2x}.$$

The transformed nonlinear ODEs are:

$$f'''+ff''-(F+1)f'^2-(M+S_p)f'-A\left(f'+\frac{1}{2}\eta f''\right)+Gr\theta\cos\alpha=0, \tag{8}$$

$$\frac{\lambda}{Pr}\theta''+MEcf'^2+f\theta'-\theta f'-A(\theta+\frac{1}{2}\eta\theta')=0. \tag{9}$$

Also, the transformed initial and boundary conditions are:

$$f(0)=0, \quad f'(0)=1, \quad \theta(0)=1 \text{ and}$$

$$f'(\infty)\to 0, \quad \theta(\infty)\to 0. \tag{10}$$

METHOD OF SOLUTION

Equations (1) to (3) with boundary conditions (4) are converted into non-dimensional equations (8) and (9) with boundary conditions (10) by applying the dimensionless quantities. MATLAB's bvp4c technique is then used to solve those equations. To apply finite difference-based solver bvp4c the equations (8), (9) and (10) are transformed respectively as follows:

$$f = y_1, f' = y_1' = y_2, f'' = y_2' = y_3, \theta = y_4, \theta' = y_4' = y_5, \tag{11}$$

$$y_3' = -y_1 y_3 + (F+1)y_2^2 + My_2 + S_p y_2 + A\left(y_2 + \frac{1}{2}\eta y_3\right) - Gry_4 cos\alpha, \tag{12}$$

$$y_5' = \frac{Pr}{\lambda}[-MEcy_2^2 - y_1 y_5 + y_4 y_2 + A(y_4 + \frac{1}{2}\eta y_5)]. \tag{13}$$

Also, the initial and boundary conditions (10) are transformed as follows:

$$y_1(0) = 0, \quad y_2(0) = 1, \quad y_4(0) = 1, \tag{14}$$

$$y_2(\infty) = 0, \quad y_4(\infty) = 0. \tag{15}$$

The above transformed results are used by the MATLAB solver bvp4c to perform the numerical computation.

RESULTS AND DISCUSSION

The aforementioned factors are taken into account when solving the problem numerically, and the results are displayed in graphs in Figures 2 to 13 for various parameters, such as the unsteadiness parameter (A), radiation parameter (N), Grashoff number (Gr) owing to heat transfer, angle of inclination (α), Eckert number (Ec), Hartmann number (M), Prandtl number (Pr), inertial parameter (F) and Porosity parameter (S_p). Table 1 depicts the effects of the various parameters on Skin friction and Nusselt number.

Figures 2, 3, 4, 5, 6 and 7 show the variation in the velocity profile for different values of A, M, S_P, F, Gr and α, respectively, while the other parameters remain unchanged. As can be seen, the velocity profile constantly rises as Gr increases and decreases as A, M, S_P, F and α increases.

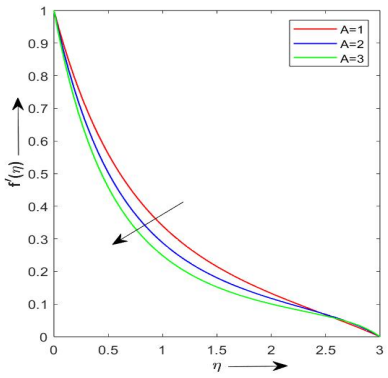

Figure 2. Velocity profile vs A

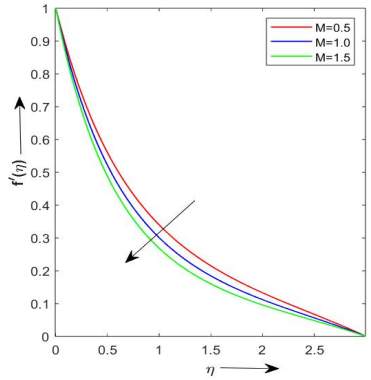

Figure 3. Velocity profile vs M

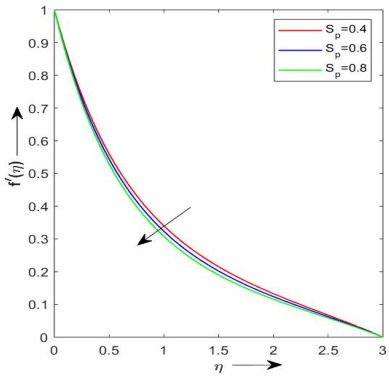

Figure 4. Velocity profile vs S_P

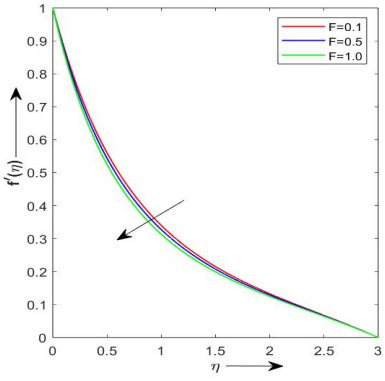

Figure 5. Velocity profile vs F

From Fig. 2 it can be noticed that the velocity profile decreases with the rise in unsteadiness parameter because the parameter reflects the temporal changes in the flow. High unsteadiness implies rapid fluctuations in the flow's velocity over time, which tends to reduce the average velocity. These fluctuations cause increased energy dissipation and mixing, leading to a reduction in the momentum of the flow. This results in a flattened velocity profile, with lower peak velocities

and a more uniform distribution across the flow's cross-section. Fig. 3 depicts that when the magnetic parameter increases, the velocity profile in a conductive fluid decreases due to the Lorentz force. This force opposes the fluid motion and generates a magnetic drag, which resists the fluid's flow. As the magnetic parameter rises, the Lorentz force becomes stronger, enhancing the drag effect. This suppresses the fluid's momentum and slows down the flow, leading to a reduction in the overall velocity profile. Additionally, the interaction between the magnetic field and the electric currents within the fluid can increase the viscous dissipation, further decreasing the velocity. Fig. 4 shows that the velocity profile decreases with a rise in the porosity parameter because increased porosity enhances the resistance to fluid flow through a porous medium. Higher porosity reduces the effective area available for fluid to pass, increasing frictional resistance and drag forces within the medium. This results in greater energy dissipation and slower fluid movement. Consequently, as the porosity parameter rises, the ability of the fluid to maintain its momentum diminishes, leading to a reduction in the overall velocity profile through the porous structure. The increased resistance also disrupts the fluid's streamline, causing a more pronounced decline in velocity. Fig. 5 depicts that the velocity profile decreases with a rise in the inertial parameter because this parameter represents the ratio of inertial forces to viscous forces in fluid flow. As the inertial parameter increases, the influence of inertial forces becomes more significant relative to viscous forces. This leads to greater momentum diffusion and turbulence, which disrupts the orderly flow and reduces the fluid's velocity. Higher inertial forces also cause more resistance against the fluid's motion, contributing to a flattening and lowering of the velocity profile. The flow's instability and increased energy dissipation further contribute to the decreased velocity as the inertial parameter rises. Fig. 6 shows that the velocity profile increases with a rise in the Grashof number due to heat transfer because the Grashof number quantifies the buoyancy forces relative to viscous forces in a fluid. Higher Grashof numbers signify stronger buoyancy forces resulting from thermal gradients. This increase in buoyancy force enhances natural convection, driving the fluid more vigorously. The intensified buoyancy-driven flow contributes to higher velocities as warmer, less dense fluid rises, and cooler, denser fluid sinks. This promotes increased movement and momentum in the fluid, steepening the velocity profile and resulting in faster overall flow, especially in regions where buoyancy forces dominate over viscous resistance. Fig. 7 depicts that with the rise in α the fluid's velocity decreases. The velocity profile decreases with a rise in the angle of inclination because the gravitational component along the inclined surface increases, which opposes the fluid flow. As the angle of inclination increases, gravity acts more strongly against the direction of the flow, creating additional resistance and reducing the fluid's momentum. This leads to a decrease in velocity, as the fluid must work harder against the gravitational pull. Moreover, the increased gravitational component enhances the vertical stratification of the fluid, leading to more pronounced variations in the velocity profile and further flattening or lowering the average velocity across the inclined plane.

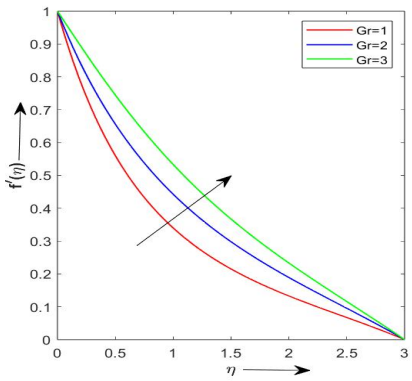

Figure 6. Velocity profile vs Gr

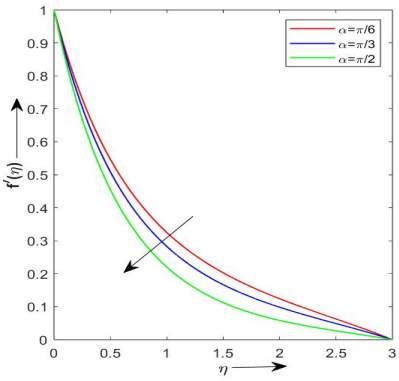

Figure 7. Velocity profile vs α

Figures 8, 9, 10, 11, 12 and 13 shows the variation in the temperature profile for different values of A, M, Pr, Ec, N and Gr, respectively, while the other parameters remain unchanged. As it can be seen that the temperature profile rises as M and Ec increases and decreases as A, Pr, N and Gr increases. Fig. 8 depicts that the temperature profile decreases with the unsteadiness parameter because this parameter reflects temporal variations in the heat transfer within the fluid. As unsteadiness increases, the temperature field fluctuates more rapidly, leading to enhanced mixing and diffusion of thermal energy. These fluctuations disrupt the temperature gradients, causing the heat to spread more uniformly throughout the fluid. This results in a more uniform and lower average temperature profile, as the thermal energy is distributed more evenly over time. Additionally, rapid changes in the flow's velocity and temperature can increase convective heat transfer, further contributing to the overall decrease in the temperature profile. Fig. 9 shows that the temperature profile increases with the magnetic parameter because the Lorentz force induced by the magnetic field slows down the fluid's motion, reducing convective heat transfer. This deceleration diminishes the ability of the fluid to carry heat away from the heated region efficiently. As a result, heat accumulates near the heat source, leading to higher temperatures in that area. Additionally, the magnetic field can induce Joule heating, where electrical currents generated by the magnetic field increase the internal energy of the fluid. This combined effect of reduced convective cooling and additional heating results in a rise in the temperature profile as the magnetic parameter increases. The temperature curve and Pr's influence are displayed in Fig. 10. As Pr increases, temperature is seen to drop, indicating a relationship between velocity and thermal

boundary layer thickness. It is believed that large values of Pr suggest a thermal diffusivity preponderance and, consequently, a smaller thermal boundary layer than a velocity boundary layer. As the surface distance grows, the temperature in the zone of unrestricted stream flow actually drops and asymptotically approaches zero. Fig. 11 shows the effect of Ec on temperature. When the fluid's temperature rises, the fluid's enthalpy decreases and its kinetic energy increases, as indicated by the rising Eckert number.

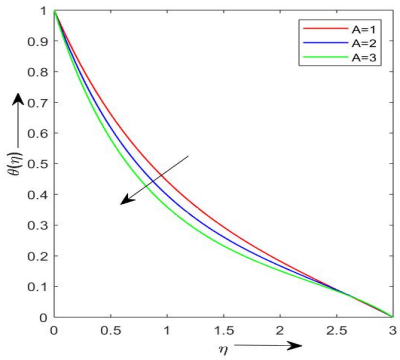

Figure 8. Temperature profile vs A

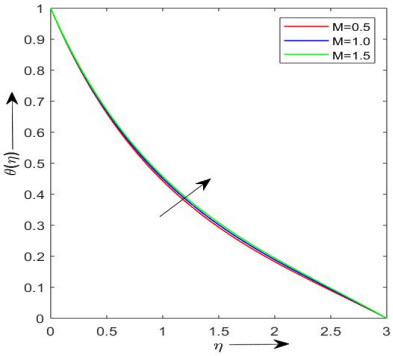

Figure 9. Temperature profile vs M

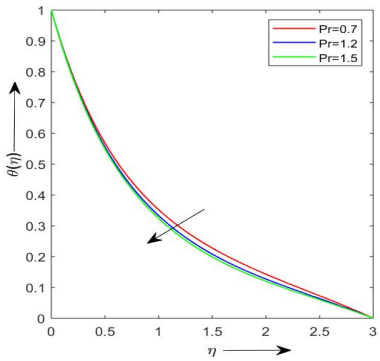

Figure 10. Temperature profile vs Pr

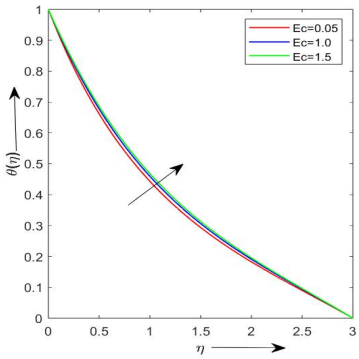

Figure 11. Temperature profile vs Ec

Fig. 12 shows how radiation affects temperature profiles. It may be observed that as N grows, the fluid's temperature drops. This is due to the fact that rising N denotes rising radiation in the thermal boundary surface where temperature description declines. Fig. 13 shows the alteration of the temperature profile with respect to the change in Gr. It is clear that the fluid's temperature decreases as Gr values rise. As the Grashof number (Gr) increases in natural convection, buoyancy forces become stronger relative to viscous forces. This results in more vigorous fluid motion and enhanced convective heat transfer. The increased fluid movement facilitates more efficient mixing of temperature within the fluid. Consequently, the temperature gradient decreases because heat is distributed more evenly throughout the fluid volume. Near the heated surface, temperatures may still be higher due to direct heat input, but as Gr increases, the overall temperature profile becomes smoother with less steep variations. This phenomenon reflects the improved thermal homogenization and heat transfer efficiency characteristic of higher Grashof numbers in natural convection systems.

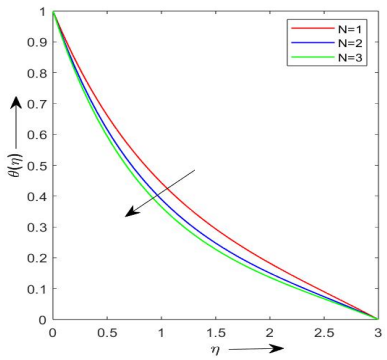

Figure 12. Temperature profile vs N

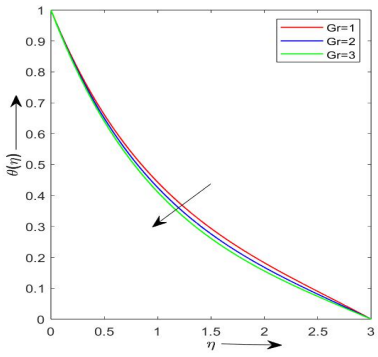

Figure 13. Temperature profile vs Gr

The effects of various parameters on the Skin friction and Nusselt number are shown in Table 1. The magnitude of the Skin friction escalates with the rise in A, M, S_p ,F, α , Pr and N, while it decreases with the rise in Gr and Ec. The magnitude of rate of heat transfer escalates with the rise in A, Gr, Pr and N, while it decreases with the rise in M, S_p F, α and Ec.

Table 1. Variation of Skin Friction and Nusselt number for A, M, S_p, F, Gr, α, Pr, Ec, N.

A	M	S_p	F	Gr	α	Pr	Ec	N	$f''(0)$	$\theta'(0)$
1	0.5	0.4	0.1	1	0	1.0	0.05	1	-1.2580	-0.8519
2									-1.5311	-1.0189
3									-1.7672	-1.1680
1	0.5								-1.2580	-0.8519
	1.0								-1.4194	-0.8473
	1.5								-1.5683	-0.8255
	0.5	0.4							-1.2580	-0.8519
		0.6							-1.3244	-0.8473
		0.8							-1.3884	-0.8430
		0.4	0.1						-1.2580	-0.8519
			0.5						-1.3507	-0.8475
			1.0						-1.4595	-0.8425
			0.1	1					-1.2580	-0.8519
				2					-0.8886	-0.8786
				3					-0.5343	-0.9079
				1	π/6				-1.3089	-0.8480
					π/3				-1.4498	-0.8369
					π/2				-1.6474	-0.8204
					0	0.7			-1.2401	-0.7199
						1.2			-1.2685	-0.9327
						1.5			-1.2823	-1.0452
						1.0	0.05		-1.2580	-0.8519
							1.0		-1.2514	-0.7862
							1.5		-1.2479	-0.7513
							0.05	1	-1.2580	-0.8519
								2	-1.2779	-1.0087
								3	-1.2872	-1.0862

CONCLUSIONS

The findings are translated into the following conclusions, which are given below:

- The velocity profile decreases with the rise in A. M. S_P, F and α.
- The velocity profile increases as Gr increases.
- The temperature profile falls with rise in A, Pr , N and Gr.
- The temperature profile escalates with the rise in M and Ec..
- The magnitude of the Skin friction escalates with the rise in A, M, S_p ,F, α , Pr and N, while it decreases with the rise in Gr and Ec.
- The magnitude of rate of heat transfer escalates with the rise in A, Gr, Pr and N, while it decreases with the rise in M, S_p F, α and Ec.

Nomenclature

a,b,c	Constant
A	Unsteady parameter (c/a),
B_0	Constant Magnetic field, (N m/A)
C_P	Specific heat at constant pressure, $(\frac{J}{kgK})$
f	Dimensionless stream function,
Ec	Eckert number,
k	Permeability of porous medium, (m^2)
k'	Forchheimer resistance factor,
q_r	radiative heat flux, (W/m^2)
M	Magnetic parameter (Hartmann number),
Pr	Prandtl number,
S_P	Porosity parameter,
N	Radiation parameter,
Nu	Nusselt number,
F	Inertial parameter,
t	Dimensionless time, (K)
T	Fluid's temperature, (K)
u	Fluid's velocity along x-direction, (m/s)
v	Fluid's velocity along y-direction, (m/s)
(x,y)	Cartesian coordinates
Gr	Grashoff number due to heat transfer

Greek Symbols

ρ	density of fluid, $(\frac{kg}{m^3})$
μ	dynamic viscosity, (Pa s)
σ_e	Electrical conductivity, $(\frac{1}{\Omega m})$
η	Dimensionless similarity variable,
ν	Kinematic viscosity, (m^2/s)
κ	Thermal conductivity, $(\frac{W}{mK})$
ψ	Stream function,
τ	Skin friction,
θ	Dimensionless temperature

Superscript

′	With regard to η, differentiation

Subscript

w	values at the plate
∞	conditions at the free stream

ORCID

Ankur Kumar Sarma, https://orcid.org/0009-0003-6209-8859; **Sunmoni Mudoi**, https://orcid.org/0009-0008-9200-5103

REFERENCES

[1] B.C. Sakiadis, "Boundary-layer behavior on continuous solid surfaces: I. boundary-layer equations for two-dimensional and axisymmetric flow," AIChE Journal, **7**(1), 26–28 (1961). https://doi.org/10.1002/aic.690070108

[2] B.C. Sakiadis, "Boundary-layer behavior on continuous solid surfaces: II. the boundary layer on a continuous flat surface," AIChE Journal, **7**(2), 221–225 (1961). https://doi.org/10.1002/aic.690070211

[3] L.J. Crane, "Flow past a stretching plate," Zeitschrift für Angewandte Mathematik und Physik (ZAMP), **21**, 645–647 (1970). https://doi.org/10.1007/BF01587695

[4] W. Banks, "Similarity solutions of the boundary-layer equations for a stretching wall," Journal de Mécanique théorique et appliquée, **2**(3), 375–392 (1983).

[5] C. Wang, "The three-dimensional flow due to a stretching flat surface," The physics of fluids, **27**(8), 1915–1917 (1984). http://dx.doi.org/10.1063/1.864868

[6] H. Andersson, "MHD flow of a viscoelastic fluid past a stretching surface," Acta Mechanica, **95**(1-4), 227–230 (1992). https://doi.org/10.1007/BF01170814

[7] E.M. Elbashbeshy, "Heat transfer over a stretching surface with variable surface heat flux," Journal of Physics D: Applied Physics **31**(16), 1951 (1998). https://doi.org/10.1088/0022-3727/31/16/002

[8] Z. Siri, N.A.C. Ghani, and R.M. Kasmani, "Heat transfer over a steady stretching surface in the presence of suction," Boundary Value Problems, **2018**, 126 (2018). https://doi.org/10.1186/s13661-018-1019-6

[9] H.I. Andersson, J.B. Aarseth, and B.S. Dandapat, "Heat transfer in a liquid film on an unsteady stretching surface," International Journal of Heat and Mass Transfer, **43**(1), 69–74 (2000). https://doi.org/10.1016/S0017-9310(99)00123-4

[10] A. Raptis, C. Perdikis, and H. Takhar, "Effect of thermal radiation on MHD flow," Applied Mathematics and Computation, **153**(3), 645–649 (2004). https://doi.org/10.1016/S0096-3003(03)00657-X

[11] A.Y. Ghaly, "Radiation effects on a certain MHD free-convection flow," Chaos, Solitons & Fractals, **13**(9), 1843–1850 (2002). https://doi.org/10.1016/S0960-0779(01)00193-X

[12] A. Ishak, et al. "MHD boundary layer flow due to an exponentially stretching sheet with radiation effect," Sains Malaysiana, **40**(4), 391–395 (2011). https://journalarticle.ukm.my/2406/1/17_Anuar_Ishak.pdf

[13] P.D. Ariel, T. Hayat, and S. Asghar, "Homotopy perturbation method and axisymmetric flow over a stretching sheet," International Journal of Nonlinear Sciences and Numerical Simulation, **7**(4), 399–406 (2006). https://doi.org/10.1515/IJNSNS.2006.7.4.399

[14] E.M. Elbashbeshy, and D.A. Aldawody, "Heat transfer over an unsteady stretching surface with variable heat flux in the presence of a heat source or sink," Computers & Mathematics with Applications, **60**(10), 2806–2811 (2010). https://doi.org/10.1016/j.camwa.2010.09.035

[15] N. Ahmad, Z. Siddiqui, and M. Mishra, "Boundary layer flow and heat transfer past a stretching plate with variable thermal conductivity," International Journal of Non-linear Mechanics, **45**(04), 306–309 (2010). https://doi.org/10.1016/j.ijnonlinmec.2009.12.006

[16] A. Ishak, "Unsteady MHD flow and heat transfer over a stretching plate," Journal of Applied Sciences, **10**(18), 2127-2131 (2010). https://doi.org/10.3923/jas.2010.2127.2131

[17] A.K. Jhankal, R.N. Jat, and D. Kumar, "Unsteady MHD flow and heat transfer over a porous stretching plate," International Journal of Computational and Applied Mathematics, **2**, 325-333 (2017). https://www.ripublication.com/ijcam17/ijcamv12n2_15.pdf

[18] N.C. Rosca, and I. Pop, "Unsteady boundary layer flow over a permeable curved stretching/shrinking surface," European Journal of Mechanics - B/Fluids, **51**, 61–67 (2015). https://doi.org/10.1016/j.euromechflu.2015.01.001

[19] M.K. Choudhary, S. Chaudhary, and R. Sharma, "Unsteady MHD flow and heat transfer over a stretching permeable surface with suction or injection," Procedia Engineering, **127**, 703– 710 (2015). https://doi.org/10.1016/j.proeng.2015.11.371

[20] I. Alarifi, A. Abo-Khalil, M. Osman, L. Lund Baloch, B.A. Mossaad, H. Belmabrouk, and I. Tlili, "MHD flow and heat transfer over vertical stretching sheet with heat sink or source effect," Symmetry, **11**(3), 297 (2019). https://doi.org/10.3390/sym11030297

[21] A.M. Megahed, N.I. Ghoneim, M.G. Reddy, and M. El-Khatib, "Magnetohydrodynamic fluid flow due to an unsteady stretching sheet with thermal radiation, porous medium, and variable heat flux," Advances in Astronomy, **2021**, 686-883 (2021). https://doi.org/10.1155/2021/6686883

[22] Y.D. Reddy, B.S. Goud, K.S. Nisar, B. Alshahrani, M. Mahmoud, and C. Park, "Heat absorption/generation effect on MHD heat transfer fluid flow along a stretching cylinder with a porous medium," Alexandria Engineering Journal, **64**, 659–666 (2023). https://doi.org/10.1016/j.aej.2022.08.049

[23] S.A.G.A. Shah, A. Hassan, H. Karamti, A. Alhushaybari, S.M. Eldin, and A.M. Galal, "Effect of thermal radiation on convective heat transfer in MHD boundary layer carreau fluid with chemical reaction," Scientific Reports, **13**(1), 4117 (2023). https://doi.org/10.1038/s41598-023-31151-4

[24] B.K. Swain, B.C. Parida, S. Kar, and N. Senapati, "Viscous dissipation and joule heating effect on MHD flow and heat transfer past a stretching sheet embedded in a porous medium," Heliyon, **6**(10), e05338 (2020). https://doi.org/10.1016/j.heliyon.2020.e05338

[25] G. Rasool, A.J. Chamkha, T. Muhammad, A. Shafiq, and I. Khan, "Darcy-Forchheimer relation in Casson type MHD nanofluid flow over non-linear stretching surface," Propulsion and Power Research, **9**(2), 159–168 (2020). https://doi.org/10.1016/j.jppr.2020.04.003

[26] P.M. Patil, N. Kumbarwadi, and A.J. Chamkha, "Unsteady mixed convection over an exponentially stretching surface: Influence of Darcy-forchheimer porous medium and cross diffusion," Journal of Porous Media, **24**(2), 29-47 (2021). https://doi.org/10.1615/jpormedia.2020026016

[27] W. Al-Kouz, A. Aissa, A. Koulali, W. Jamshed, H. Moria, K.S. Nisar, A. Mourad, *et al*., "MHD Darcy-Forchheimer nanofluid flow and entropy optimization in an odd-shaped enclosure filled with a (mwcnt-Fe_3 O_4/water) using galerkin finite element analysis," Scientific Reports. **11**, 22635 (2021). https://doi.org/10.1038/s41598-021-02047-y

[28] B. Mandal, K. Bhattacharyya, A. Banerjee, A.K. Verma, and A.K. Gautam, "MHD mixed convection on an inclined stretching plate in darcy porous medium with soret effect and variable surface conditions," Nonlinear Engineering, **9**, 457–469 (2022). https://doi.org/10.1515/nleng-2020-0029

[29] A.K. Sarma, "Unsteady radiative MHD flow over a porous stretching plate," in: *Modeling and Simulation of Fluid Flow and Heat Transfer*, (CRC Press, 2024), pp. 96–109. https://doi.org/10.1201/9781032712079-7

[30] A.K. Sarma, and D. Sarma, "MHD flow in free convection over an exponentially stretched sheet submerged in a double-stratified medium," International Journal of Ambient Energy, **45**(1), 2356060 (2024). https://doi.org/10.1080/01430750.2024.2356060

РАДІАЦІЙНИЙ ЕФЕКТ НА НЕСТАЦІОНАРНИЙ МГД-ПОТІК ДАРСІ ФОРХГЕЙМЕРА ПО ВЕРТИКАЛЬНОМУ ПОХИЛОМУ ЛИСТУ, ЩО РОЗТЯГУЄТЬСЯ У ПРИСУТНОСТІ ПОРИСТОГО СЕРЕДОВИЩА

Анкур Кумар Сарма[a,e], Сунмоні Мудоі[a], Палаш Нат[b], Панкадж Каліта[c], Гауараб Бардхан[d]

[a]Факультет математики, університет Коттона, Пан Базар, Гувахаті, Індія

[b]Кафедра математики, коледж Барбаг, Калаг-781351, Індія

[c]Кафедра математики, коледж ADP, Нагаон-782002, Індія

[d]Факультет математики, коледж Тягбір Хем Баруа, Джамугуріхат, Сонітпур, 784189, Індія

[e]Факультет математики, Коледж Баосі Баніканта Какаті, Нагаон, Барпета-781311, Індія

У цьому дослідженні розглядається, як випромінювання та тепло переміщуються через двовимірний, нестаціонарний МГД-потік Дарсі-Форхгеймера, який протікає через пористу розтягнуту вертикально нахилену пластину, до якої прикладено поперечне магнітне поле. Ми використовуємо підхід MATLAB bvp4c для чисельного перетворення нелінійних PDE керуючого граничного шару, які є рівняннями в часткових похідних, у набір нелінійних ODE, які є звичайними диференціальними рівняннями, використовуючи перетворення подібності. Ми кількісно оцінюємо профілі швидкості та температури за допомогою графіків, які представляють різні характеристики проблеми, включаючи нестаціонарність, число Прандтля, магнітне поле, число Грашоффа, параметр випромінювання та число Екерта. Таблиці ілюструють вплив на тертя шкіри (τ) і число Нуссельта (Nu). Профіль швидкості зменшується зі збільшенням магнітних та інерційних параметрів, а профіль температури зменшується зі збільшенням параметрів випромінювання.

Ключові слова: *магнітогідродинаміка (МГД); випромінювання; Дарсі-Форххаймер; пористе середовище; теплообмін; нестабільність*